Simulation of Blast Load Reduction on Walls with Foamed Concrete Boards

Yijian Shi, PhD
ZASA - Logan, Zodiac Aerospace
*jack.shi@zodiacaerospace.com*

Abstract

A foamed concrete board (FCB), often used as an insulation layer in structures, has been used to study blast attenuation. A LS-DYNA® explicit solver chosen as a simulation tool reveals the physics of pressure waves, which transfer through materials, and internal stress in detail. The effectiveness of blast attenuation is measured by the reduction of peak pressure acting on a rigid wall (RW) that is immediately behind the FCB. According to the simulation results, the internal stress in FCB can reach much higher than its static strength under the blast loading. The internal stress is a function of not only material's failure stress and strain/deformation, but also its density, elastic modulus, plastic properties, internal speed, and acceleration. This observation might result in the difficulty to measure the internal stress or load, because load cells and strain gages traditionally only measure the strain or deformation, which can be converted to stress statically. The simulation results indicate that the higher the pressure of the blast than the strength of FCB, the higher the reduction for the peak pressure on RW is. On the contrary, if the pressure of a blast is lower than or about the strength of FCB, there is no reduction of the peak pressure on RW, rather than a significant increase. It seems that the increase is getting relatively larger as the pressure of the blast decreases.

Introduction

A foamed (or cellular) concrete board (FCB) has been widely used for thermal insulation on not only internal but also external walls (see Figure 1) of buildings, especially in some Asian countries, because FCB has very low thermal conductivity. Although FCB is a type of concrete, it is much lighter than a regular concrete wall (RCW). Since the RCW takes loads in structure, FCB can be used solely for the purpose of insulation. The advantages of FCB are light weight, easy handling, and low cost due to small quantity of cement materials consumed. In comparison to other types of more inexpensive insulation materials, such as polymeric foam boards, FCB is inorganic, incombustible (no flame, no toxic fame, no smoke) and worked well under high temperature.

(a)
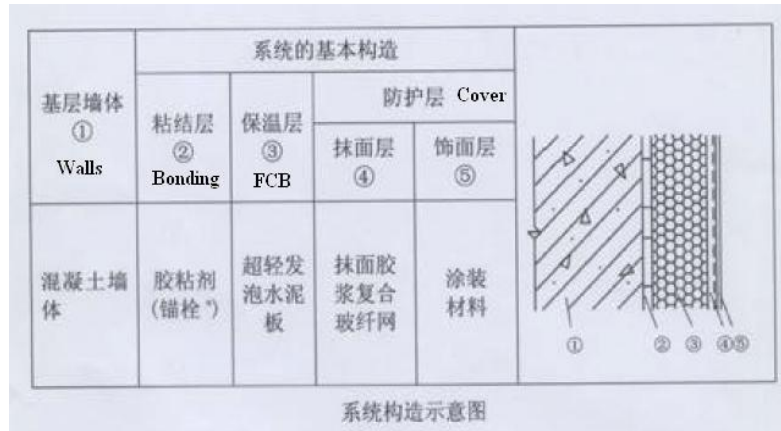
(b)

Figure 1   An Example of FCB Application. (a) FCB used as exterior walls; (b) Wall structure layout. (Courtesy of Beijing Polar Bear Construction Materials Co.)

As production technology of foamed or cellular concrete (CC) is maturing further, the making of FCB becomes easier and more inexpensive. The advantages of FCB have been gradually recognized and have become more widely used in construction. One of its applications is shown in Figure 1, in which FCB is used as an exterior wall. Regarding CC and its applications, it seems that there are more application standards in some Asian countries. Nevertheless, the ACI (American Concrete Institute) has published a guidance[1] for CC that has a density of more than 50 (lbs/ft).

With the growing concerns on building venerability subjected to explosions, researchers have carried out a number of tests and simulations[3-7] to study the blast effect, and to reduce the effect by strengthening structures. ACI has published a report for the design of concrete structures for blast effects[2].

Besides strengthening structures, some published papers have studied the method of using weak materials[8-17] to reduce blast effect. These weak materials include polymeric foam, alumina foam, CC, and others. Weak CC has been used functionally like a sacrificial cladding layer to reduce the damage from blast pressure on a protected structure.

When the blast wave travels through the materials, physics and internal mechanism of pressure waves may not be revealed by simplified analytical models with assumptions or by testing, because of the measurement restrictions and difficulties to control conditions. A good FEA simulation, which can better control conditions and can have better repeatability, may be able to overcome the shortfalls. The LS-DYNA® explicit solver, as an engineering tool, is selected in the study. The blast effects on CC walls, especially on FCBs, have not been fully investigated in detail using this tool. The potential benefits from FCB installations, when buildings are exposed to blasts, will be studied in this paper with LS-DYNA®.

Based on the mechanical properties of FCB, the blast loads on the walls with and without FCB will be simulated. Study on effects of strength of the blast will be presented. The results will

reveal that the reduction of the blast loads on the walls can be an additional advantage, besides the factors previously discussed, such as thermal conductivity, combustibility, cost, and weight.

Simulation Condition

To study the potential benefit of an insulation layer made of FCB to reduce the damage on a building structure under blast pressure, the following scenario is considered. Assume an explosive charge is detonated in front of the FCB which is unconstrained, as illustrated in Figure 2. The blast wave directly hits the FCB that could be damaged. The pressure wave transfers through the FCB and hits a rigid wall (RW). The reaction force is generated by the RW against the incoming blast pressure. The potential reduction on the reaction force, as a benefit of the existence of the FCB, is studied here. The reaction force can also be expressed as pressure on the RW, defined as
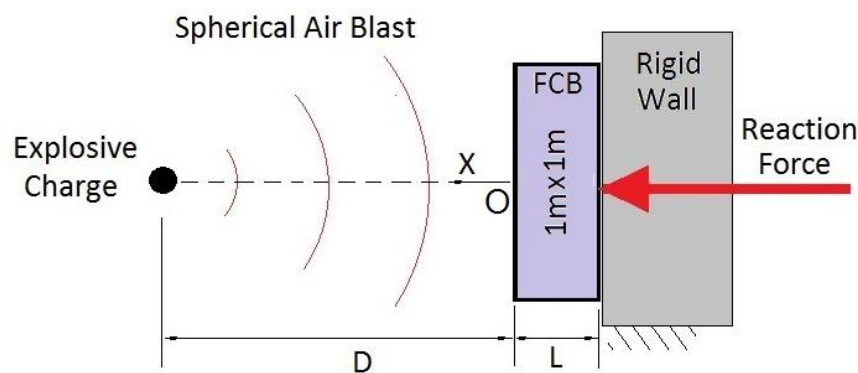
(Pressure on the RW) = (Reaction Force)/(Area of FCB)

Figure 2   Simulation Conditions and Design

The simulation is conducted with LS-DYNA® Version 8.0. The default condition is as follows: FCB was modeled by Material Type #63 (MAT_CRUSHABLE_FOAM), using 0.1 (m) thickness (L) of 1 (m) x 1 (m) size. The origin (O) of the x-axis is located at the center of FCB. The explosive charge weighs W (kg) at distance D, away from front face of CW. A spherical free-air burst is used to generate blast pressure. Solid elements with Lagrangian mesh size 0.025 (m) x 0.025 (m) x 0.025 (m) are used. Assume all simulations are based on the default case, unless changes are specified.
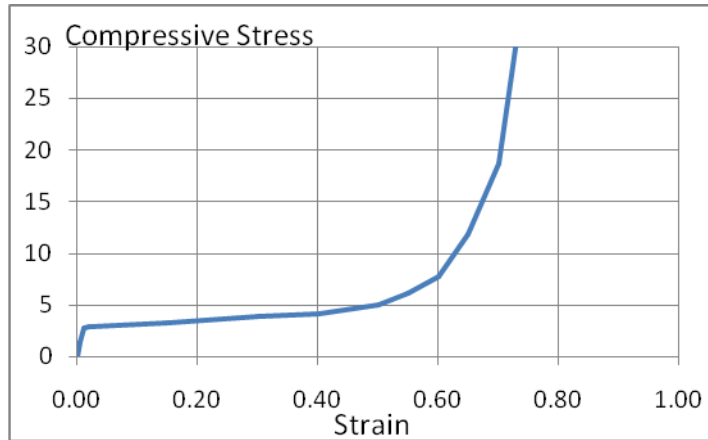
Figure 3   Compressive Strength of FCB

The compressive strength of FCB material is shown in Figure 3, which clearly shows the typical characteristics of a crushable foam material. Within very little deformation under compression, the material elastically reaches the failure point at about 2.5 pressure unit. Then, the compressive strength stays in a plateau or a relative stable value (from 2.5 up to 5.0 pressure unit) within a large range of strain, and the compressed material experiences a plastic progressive failure. At around 60% strain, the material is at a compaction phase and is quickly getting denser and harder.

Blast Effect on FCB

For the default condition, the simulated result of pressure contour on a quarter of model is shown in Figure 4. The defined Nodes #1 - #5 and Elements #1 - #4 at the center of FCB along x-direction, which is aligned with the blast charge, will be discussed later.
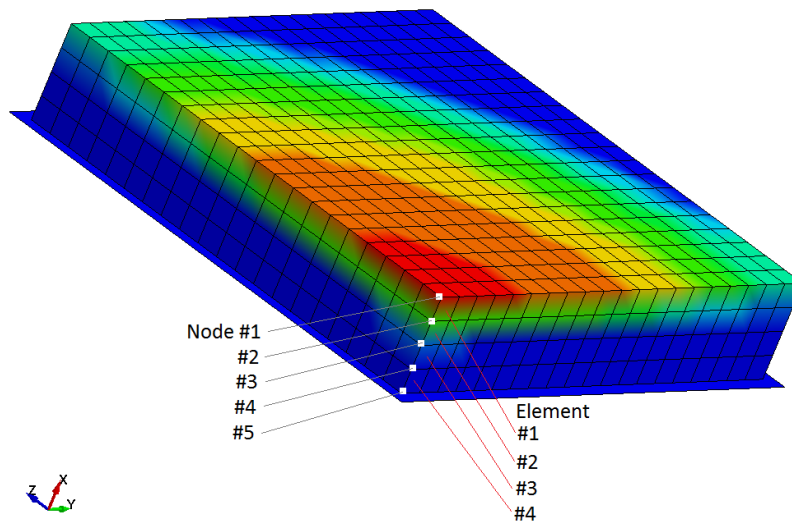

Figure 4   Pressure Contour at Time = 0.003 and Definition of Nodes and Elements

If there is no FCB, the pressure at the front of the shock wave is directly loaded on RW. According to the simulation results in Figure 5, the peak pressure at the front of the shock wave

reaches 8.5 pressure unit at time=0.003 (s). However, because of the existence of FCB, peak pressure on RW reduces to about 6.6 pressure unit at 0.0036 (s), which is about a 22% reduction on the peak pressure of the shock wave. By integrating the impulse (Pressure*time), the total pulses for the shock wave and on RW, which are equal to the areas under the pressure curves in Figure 5, are 0.0172 pressure unit*second and 0.0174 pressure unit*second, respectively. It seems that the impulse on RW is slightly larger than the one for shock wave.
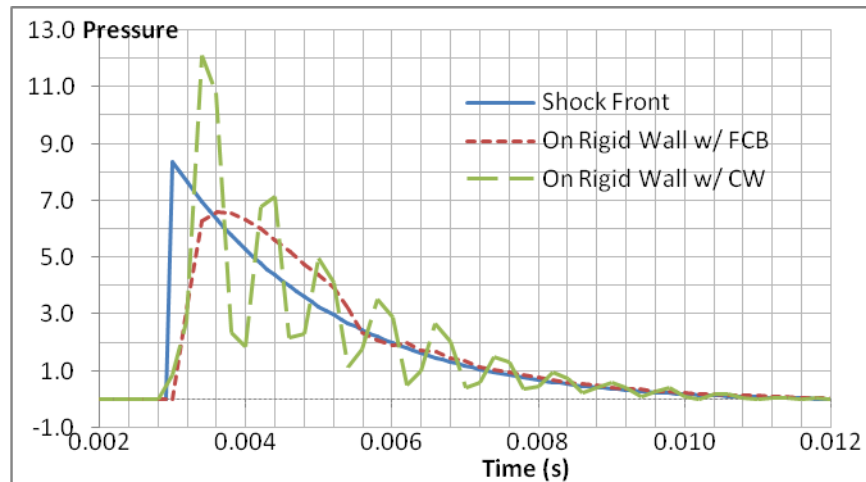

Figure 5   Simulated Pressure History

In addition, the results also indicate that the pressures for the shock wave and on RW at time < 0.006 (s) are significantly higher than the failure strength (2.5 pressure unit) of FCB, as shown in Figure 3. Based on statics principles, the relationship of FCB stress and strain should follow the curve in Figure 3. Or FCB should be compressed significantly in the plateau phase, or even fully compacted, to balance the pressures. However, according to the results of effective plastic strain for Elements #1 - #4 shown in Figure 6 and x-displacement for Nodes #1 - #5 in Figure 7, the maximum values of the effective plastic strain and x-displacement are less than 10% and 17% (=0.017/0.1), respectively, at which the material stress found in Figure 3 is only about a fraction of the pressures. Actual strain rate at local between nodes in x-direction, presented in Figure 8, is calculated based on the results in Figure 7. For time < 0.006 (s), the actual strain rate is less than 11%. In additional, checked into detailed stresses inside elements in Figure 9, the stresses in x-direction at the time range of 0.003 - 0.005 (s) can reach up to 6.5 pressure unit, which are, again, much higher than FCB stress associated with the strain in that time range.
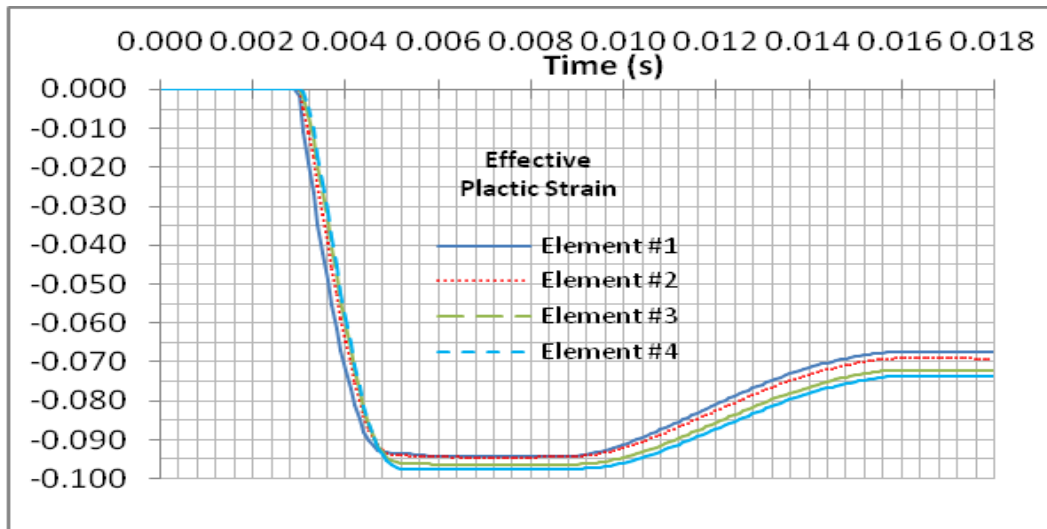
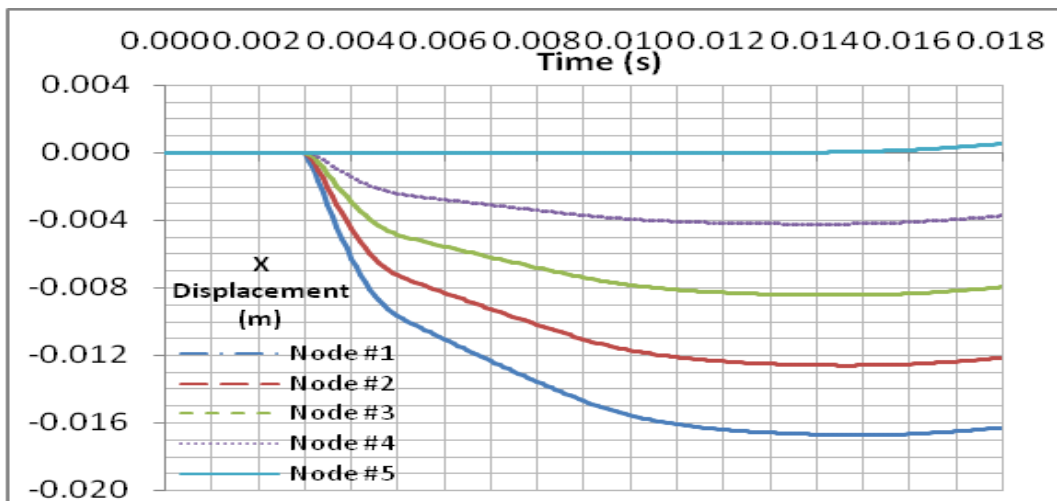Figure 6   Effective Plastic Strain in Elements #1 - #4
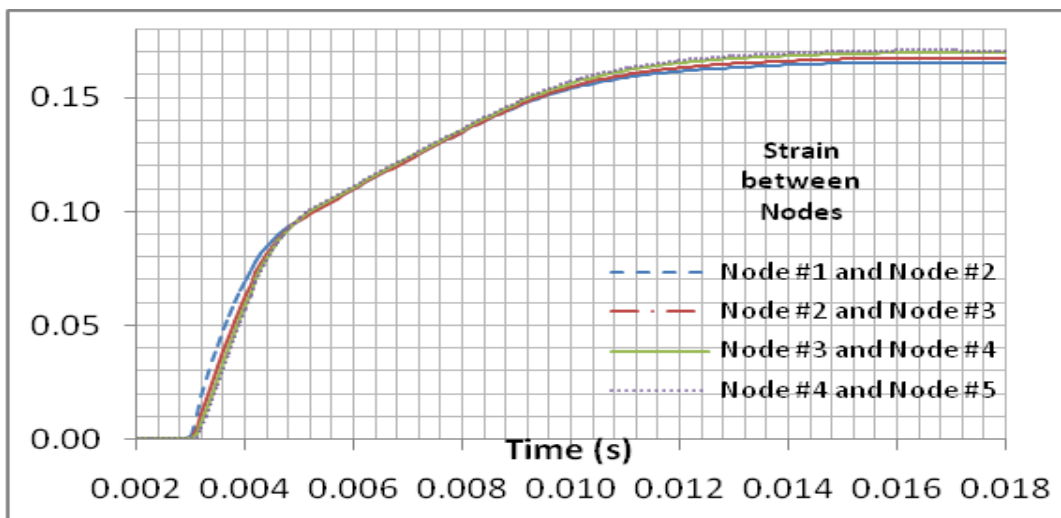

Figure 7   Displacement of Nodes #1 - #5

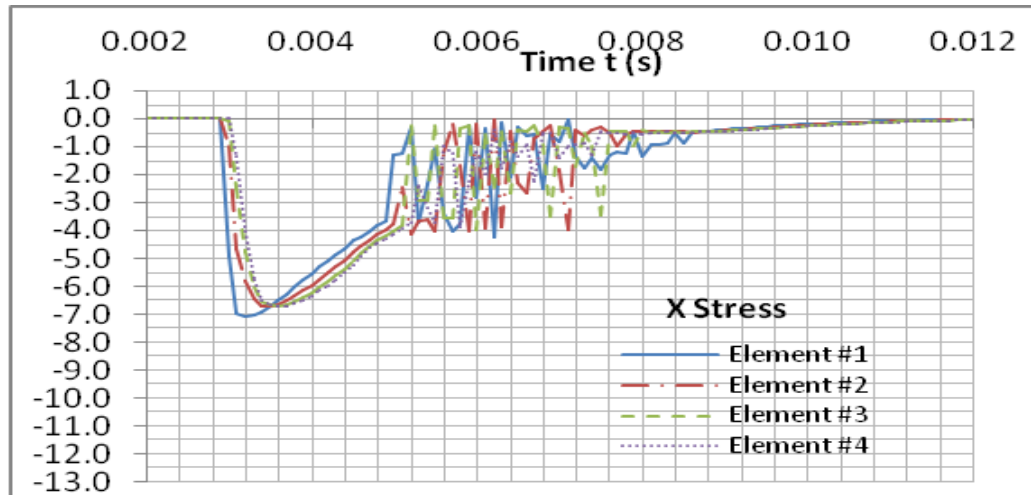Figure 8   Local Strain Between Adjacent Nodes

Figure 9   Internal Stress of Elements #1 - #4 in x-Direction

The question of why FCB, such a fragile material, can sustain such high stress now arises. An attempt to explain the phenomenon is as follows. Based on statics, it may not be rational. However, it can be explained in the dynamics arena. Figure 10 illustrates a pressure wave travels through materials at the speed V0 at an instant time t. Pressure, temperature, density, and speed before and after the front of the pressure wave are P1, T1, $\rho1$, V1 and P2, T2, $\rho2$, V2, respectively. Based on the mass conservation principle, before and after the front,

$$\rho1*A*(V0-V1)*\Delta t = \rho2*A*(V0-V2)*\Delta t$$

Or

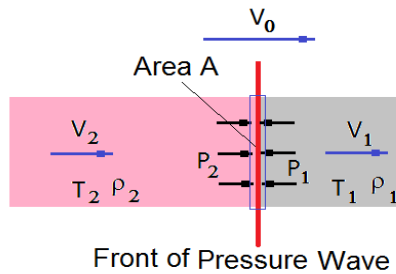$$\rho1*(V0-V1) = \rho2*(V0-V2) \tag{1}$$

Figure 10   Illustration of Pressure Wave Traveling through a Material

Based on the momentum conservation principle on the front,

$$(P2*A - P1*A)*\Delta t = \rho1*(V0-V1)*\Delta t*A*(V2-V1)$$

Then

$$(P2 - P1) = \rho1*(V0-V1)*(V2-V1) \tag{2}$$

Based on Equation (1), Equation (2) can also be rewritten as

$$(P2 - P1) = \rho2*(V0-V2)*(V2-V1) \tag{3}$$

Therefore

$$\Delta P = \rho \, V \, \Delta V \tag{4}$$

This equation can usually be seen in some textbooks. ΔP and ΔV are pressure and speed increases or gradients after the front. ρ and V are material density and associated relative speed to the front. According to Equation (4), the pressure can increase or decrease at any instant time, or there is a pressure gradient (or a pressure wave) between materials delineated by the front, the magnitude of which is determined by (1) a density of any one of the materials, (2) a material's relative speed in the direction of the pressure gradient, which may be functions of the elastic modulus or plastic properties of the material, to the front of pressure wave, and (3) a speed change through the front in the direction of the pressure gradient.

Decreasing the relative speed can also decrease the pressure. Therefore, when a speed change driven by a pressure gradient is high enough inside a material, the internal stress of the material may not be mainly limited by the static strength of the material, even though the static strength of the material can contribute to both P2 and P1.

Furthermore, Equation (4) considers pressure/stress in a spatial domain, or at different locations in a material, rather than at the same location for statics. For static case, $V=0$ or speed is constant ($\Delta V=0$), and according to Equation (4), $\Delta P = 0$, which means the pressure/stress in the speed direction is constant everywhere inside a material. Then P or σ follows statics principle, or Hooke's theorem

$$\sigma = E * \varepsilon$$

σ, E, and ε are stress, modulus, and strain. Therefore, Equation (4) is in agreement with statics principle.

Figure 11 shows that all nodes from Nodes #1 to #4 have certain speed in x-direction at the time range of 0.003 - 0.005 (s), except for Node #5 located on RW that has zero speed. Speed differences between two adjacent nodes in Figure 12 can be observed, which means there is a speed gradient inside FCB. The acceleration rate in x-direction in Figure 13 and its close-up view in Figure 14 further confirm that all material inside FCB at the time rage of 0.003 - 0.005 (s) is under certain acceleration or deceleration. According to Equation (4), the internal stress of FCB should increase at the acceleration zone and decrease at the deceleration zone, if the speed is positive.
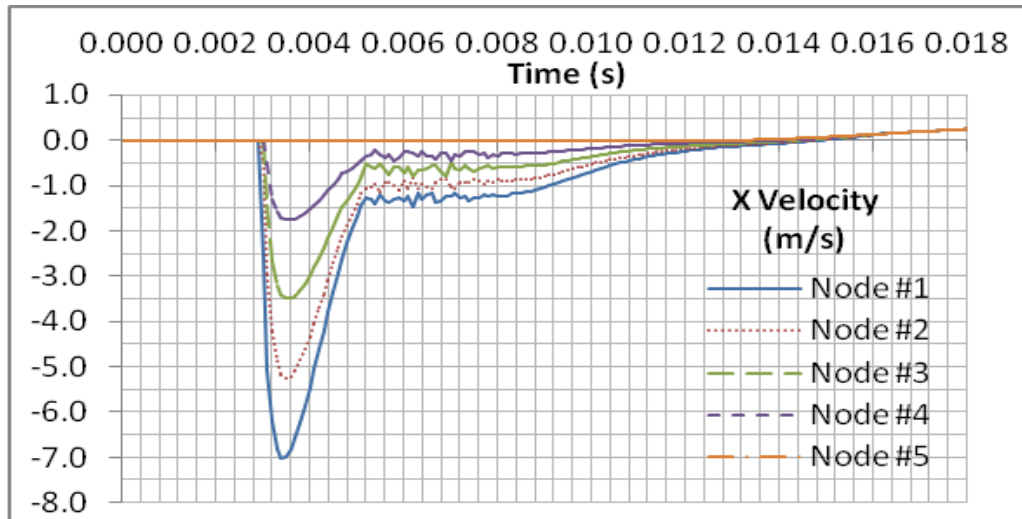
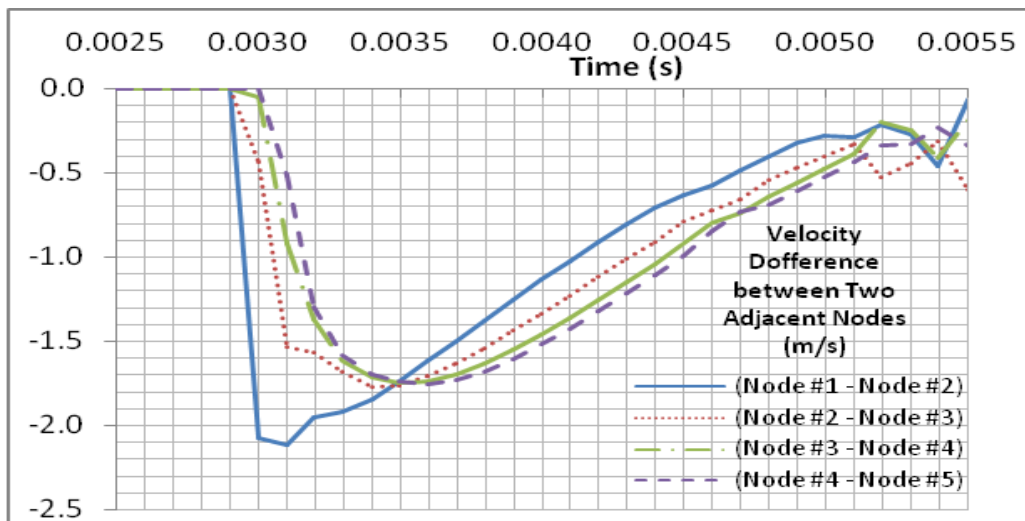Figure 11   Velocity of Nodes #1 - #5 in x-Direction

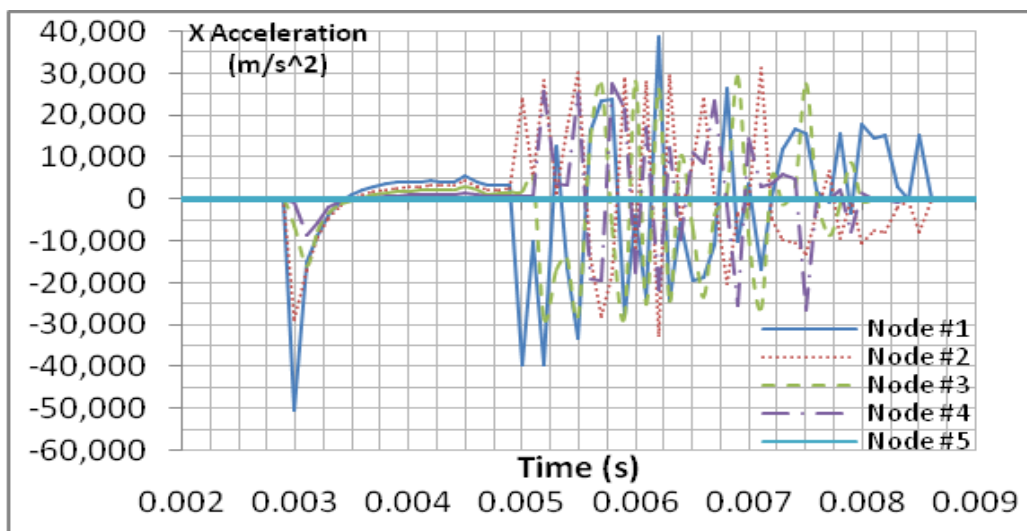Figure 12   Velocity Difference between Two Adjacent Nodes

Figure 13   Acceleration Rate of Nodes #1 - #5 in x-Direction

Let's focus on Node #4 in Figure 14, which is the closest one to RW or immediately above RW. Its acceleration rate reaches zero at about time=0.0035 (s), or the rate is negative at time < 0.0035 (s). Based on the knowledge learned from Equation (4), the internal stress should increase for time < 0.0035 (s) and decrease for time > 0.0035 (s), which is consistent with the observation from Figure 9 that the stress in x-direction reaches a peak value. Be aware that the negative value of acceleration represents the case of an acceleration because the velocity shown in Figure 11 is negative. Remember that the peak pressure on RW in Figure 5 is about time=0.0036 (s), a very short delay in comparison to time=0.0035 at which the stress in x-direction reaches the peak value for Element #4. However, from Element #1 to #4, the time at which acceleration reaches zero is delayed. Element #4 is not exactly located in RW even though Element #4 is the closest element to RW, which means that the very short latency is most likely. In other words, the pressure peak on RW in time delay from 0.0035 (s) to 0.0036 (s) can be explained.
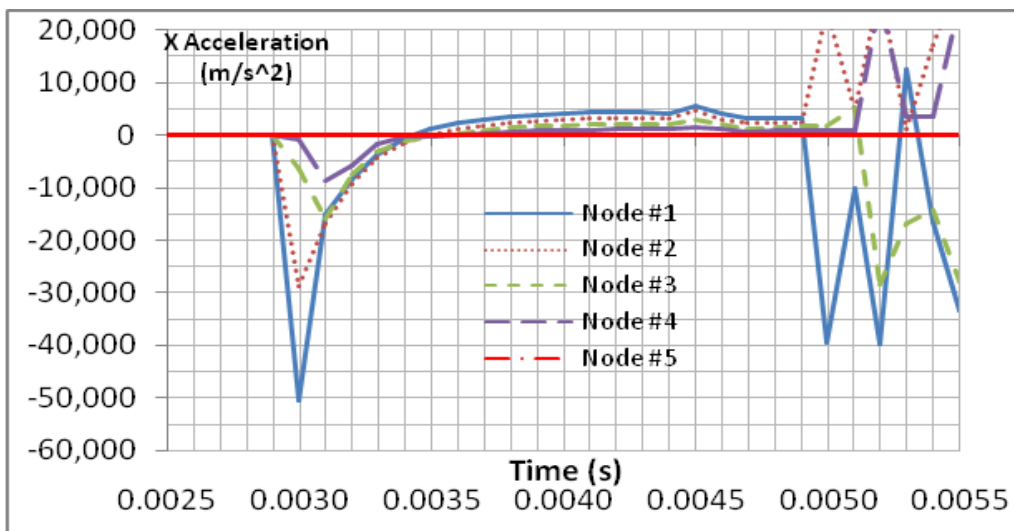

Figure 14   Close-Up View of Acceleration Rate of Nodes #1 - #5 in x-Direction

At around time=0.005 (s), the pressure built by reflected pressure waves decreases to zero. The strain is finally large enough to be well in a plastic plateau, and the associated static stress is about the same as the blast pressure. According to Equation (4), speed doesn't change and should be at a constant. If the speed reaches zero before the blast pressure reduces to the level equal to the static stress, the blast effect should be over at this instant. However, the crushed material is still at a relative speed of about 0.3 (m/s) between adjacent nodes (See Figure 12).

For time>0.005 (s), because the static stress relatively doesn't increase much and the decrease of the blast pressure is slow, possible balance between the static stress and the blast pressure can exist for a period of time, and the speed inside the crushed material is relatively close to a constant. This results in that the deformation continues to grow for a relatively longer period of time. Governed by Equation (4), the continuing decrease of the blast pressure eventually results in the speed's decrease to zero at around time=0.015 (s) (See Figure 12); meanwhile, the pressure on RW decreases to zero, too.
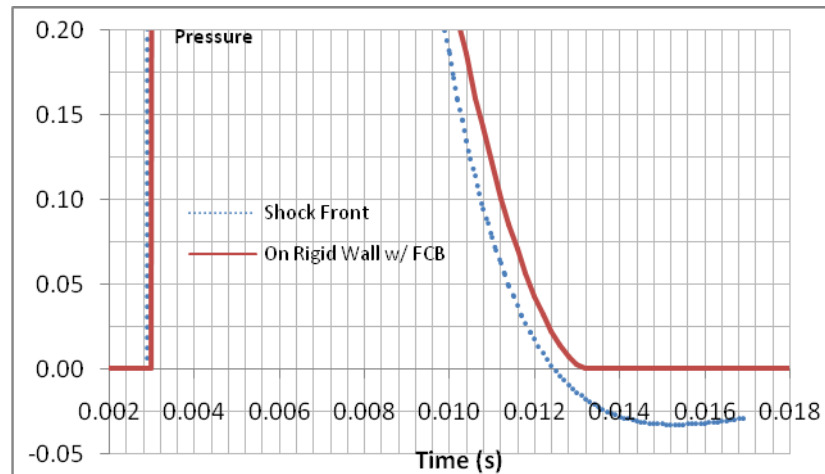
Figure 15   Close-Up View at the End of Blast Wave

For time > 0.015 (s), because the value of the blast pressure plotted in Figure 15 becomes negative, the material begins to move away from RW, which can be observed in Figure 7 and Figure 11. In addition, if the compressed material has the resilience of rebounding, the speed of moving away from RW can be boosted. Remember that at the beginning of this discussion, the pulse on RW was a little bit higher than the one for blast pressure that has been mentioned. The phenomenon could be caused by the combination of the FCB's absorption of the negative pressure of the blast and the additional negative momentum that is generated from the material moving away from RW due to rebounding . Moreover, the similar phenomenon revealed in test results[11], at which more momentum has been transferred to a back plate if a cladding layer existed, can be explained, too.

Two important points can be explained so far: (a) The reduction of the peak pressure on RW can be understood with Equation (4), and (b) The internal stress in FCB can be significantly higher than its static strength. The dynamic behaviors of a fragile material under the existence of acceleration and speed can be different from the material under static conditions. The results show that the internal stress is a function of not only failure stress and strain/deformation, but also density, elastic modulus, plastic properties, speed, and acceleration. This may result in the difficulty to measure the internal stress or load, because load cells and strain gages traditionally measure the strain or deformation only, and then statically convert it to stress based on Hooke's principle

$$\sigma = E * \varepsilon$$

For example, assume that a strain patch is used to measure the strain in x-direction for the default case. At time=0.0036 (s), the measured strain from the strain patch should be about 3 - 5% according to Figure 8. Then, using Hooke's principle or checking up the value in Figure 3, the internal stress in x-direction should be about 2.5 pressure unit. However, at that moment, the internal stress in x-direction in Figure 9, and the pressure on RW as well in Figure 5, have reached their peak values, about 6.6 pressure unit.

It's worth to mention that using the static principles to design a measurement means[16], in a test of blast attenuation, is still common. If the strain patch is installed on the test section of a sample, it's measuring a local strain. If the strain patch is on a strong supportive base, its calibration can

be difficult due to the boundary effect, which can result in a value of uncertainty such as a case of reflected pressure/stress back and forth. In addition, its measurement may not only have a time delay, but it may also include additional reflected pressure/stress from the base material. The results based on the static means may carry a significant error.

The effectiveness of FCB on the reduction of peak pressure can be further confirmed in comparison to the case of replacing FCB by a concrete wall (CW) with the same thickness (L). CW has about 10 times density of FCB's and 620 pressure unit of yield strength. Based on the result shown in Figure 5, the peak pressure on RW for the case with CW is 12.1 pressure unit at time=0.0034 (s), which is not reduced by CW, rather increased significantly by about 42%, at least for the specific case if it's not enough to be conclusive in general.

Even though the peak pressure is higher, it is still small in comparison to the yield strength of CW. The nature of pressure oscillation in Figure 5 results from the shock waves bounced back and expansion waves sweeping forth against RW. Nevertheless, the reflection of the first series of shock waves results in the first peak pressure on RW, which is much higher than the blast pressure at that moment. Then, the first series of expansion waves generate and sweep towards RW, resulting in the first valley pressure on RW in Figure 5. Furthermore, it seems undeniable that FCB is much better at significantly reducing the effect of the shock wave, in comparison to CW.

Effects of Blast Strength

This section discusses the blast attenuation affected by different blast strengths. The pressure of a blast front is associated with the charge weight and distance from an object, which is well understood[2]. Besides the default case, additional four different pressures of the blast strength, achieved by varying distance and weight, are considered and named as Weaker, Weak, Strong, and Stronger in Table 1.

Table 1   Simulation Results for Different Blast Strength

Condition	Weaker	Weak	Default	Strong	Stronger
Charge Weight	W	W	W	2W	4W
Distance	2D	1.5D	D	D	D
Blast Peak Pressure	1.62	3.00	8.50	16.40	32.00
Peak Pressure on RW	2.15	3.43	6.60	11.60	22.16
Peak Deduction	-32.84	-14.40	22.35	29.27	30.75

Simulation results for all 5 cases are summarized in Table 1 and plotted in Figures. 16 - 17. The higher the pressure of a blast than the strength of FCB, the higher the reduction for the peak pressure on RW is. On the contrary, when the pressure of a blast is lower than or close to the strength of FCB, there is no reduction for the peak pressure on RW. Instead, there is a significant increase. It seems that the increase is relatively getting bigger as the pressure of a blast decreases.
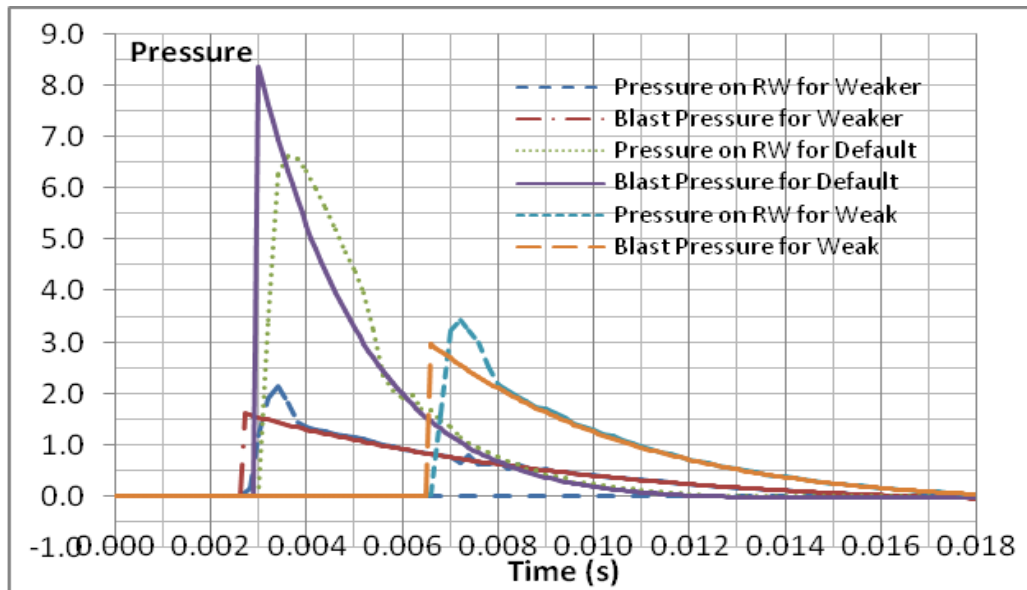
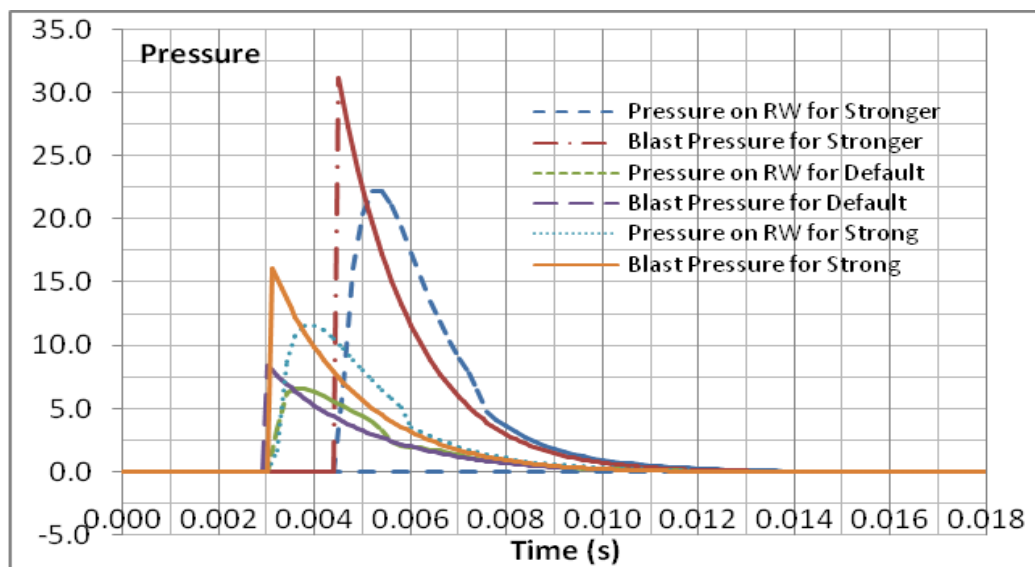Figure 16   Simulation Results for Weak and Weaker Cases

Figure 17 Simulation Results for Strong and Stronger Cases

However, for a low pressure of a blast wave, the attenuation may not be needed, or the peak pressure on RW may not be high enough to be a big concern, anyway.

In addition, it is worth to point out that the findings seem contradictory to the results from some other studies[16] which most likely were based on static principles. This paper is not going to discuss the difference in detail.

Conclusion

The potential benefits from FCB installations, when buildings are exposed to blast, have be studied. The preliminary conclusions are as follows:

1. The reduction of the peak pressure on RW can be explained with Equation (4).

2. The internal stress in FCB can reach much higher than its static strength. The dynamic behaviors of a fragile material under existence of acceleration can be different from the static ones. The internal stress is a function of not only failure stress and strain/deformation, but also density, elastic modulus, plastic properties, speed, and acceleration. This may result in the difficulty to measure the internal stress or load, because load cells and strain gages traditionally measure the strain or deformation only, and then statically convert it to stress based on Hooke's principle $\sigma = E * \varepsilon$.

3. For the default case, FCB can reduce the peak pressure of the shock wave. The effectiveness of FCB is further confirmed in comparison to the case of replacing FCB by CW. For much higher pressure of a blast than the strength of FCB, the reduction for the peak pressure on RW is higher. On the contrary, when the pressure of a blast is lower than or around the strength of FCB, there is no reduction for the peak pressure on RW, and instead, an increase in peak pressure may occur. For the low blast case, it seems that the peak pressure increase gets bigger as the pressure of a blast decreases. However, for the low pressure of a blast wave, the attenuation may not be needed, or the peak pressure on RW may not be high enough to be a big concern, anyway.

The study in the report uses the LS-DYNA® explicit solver. The conclusions of course rely on the assumptions that the explicit solver, element formulation, mesh, and the material model work well with blast waves. Furthermore, the conclusions may need verifications by effective testing with the capability of measuring true load/pressure.

References

[1] ACI Committee 523, "Guide for Cast-in-Place Low Density Cellular Concrete," American Concrete Institute, Farmington Hills, MI, ACI 523.1R-06, August 2006.
[2] ACI Committee 370, "Report for the Design of concrete Structures for Blast Effects," American Concrete Institute, Farmington Hills, MI, ACI 370R-14, July 2014.
[3] Nash, P. T.; Vallabhan, C. V. G.; and Knight, T. C., "Spall Damage to CWs from Close-In Cased and Uncased Explosions in Air," ACI Materials Journal, November-December 1995, pp. 680-687.
[4] Thiagarajan, G., and Johnson, C. F., "Experimental Behavior of Reinforced Concrete Slabs Subjected to Shock Loading," ACI Materials Journal, November-December 2014, pp. 1407-1418.
[5] Crawford, J. E.; Malvar, L. J.; Wesevich, J. W.; Valancius, J.; and Reynolds, A. D., "Retrofit of Reinforced Concrete Structures to Resist Blast Effects," ACI Materials Journal, July-August 1997, pp. 371-377.
[6] Orton, S.; Jirsa, J. O.; and Bayrak, O., "Carbon Fiber-Reinforced Polymer for Continuity in Existing Reinforced Concrete Buildings Vulnerable to Collapse," ACI Materials Journal, September-October 2009, pp. 608-611.
[7] Soroushian, P., and Obaseki, K., "Strain Rate-Dependent Interaction Diagrams for Reinforced Concrete Sections," ACI Materials Journal, January-February 1986, pp. 108-116.
[8] Guruprasad, S., and Mukherjee, A., "Layered sacrificial claddings under blast loading," Part I - analytical studies, International Journal of Impact Engineering, 24 (2000) 957-973.
[9] Guruprasad, S., and Mukherjee, A., "Layered sacrificial claddings under blast loading," Part II - experimental studies, International Journal of Impact Engineering, 24 (2000) 975-984.
[10] Li, Q.M., and Meng, H., "Attenuation or enhancement—a one-dimensional analysis on shock transmission in the solid phase of a cellular material," International Journal of Impact Engineering, 27 (2002) 1049–1065.
[11] Hanssena, A.G.; Enstockb, L.; and Langseth, M., "Close-range blast loading of aluminum foam panels," International Journal of Impact Engineering, 27 (2002) 593–618.

[12] Ma, G.W., and Ye, Z.Q., "Energy absorption of double-layer foam cladding for blast alleviation," International Journal of Impact Engineering, 34 (2007) 329–347.

[13] Ma, G.W., and Ye, Z.Q., "Analysis of foam claddings for blast alleviation," International Journal of Impact Engineering, 34 (2007) 60–70.

[14] Mostafa, H. E.; El-Dakhakhni, W. W.; and Mekky, W., "Use of reinforced rigid polyurethane foam for blast hazard mitigation," Journal of Reinforced Plastics and Composites, 29(20) 3048–3057.

[15] O'Neil, E. F.; Shen, W.; Jennings, H. M.; Thomas, J. J.; and Cummins, T., " Development of Frangible Concrete to Reduce Blast-Related Casualties," ACI Materials Journal, January-February 2012, pp. 31-40.

[16] Nian, W.; Subramaniam, K. V.; and Andreopoulos, Y., "Experimental Investigation of Blast-Pressure Attenuation by Cellular Concrete," ACI Materials Journal, January-February 2015, pp. 21-28.

[17] Mousa, M. A., and Uddin, N., "Response of CFRP/AAC Sandwich Structures under Low-Velocity Impact," ACI Materials Journal, January-February 2014, pp. 99-110.